

Quaternary Tellurides with Different Valent Ge Centers:
Cs₂Ge₃M₆Te₁₄ (M = Ga, In)Cheng-Yi Zhang,^{†,‡} Liu-Jiang Zhou,^{†,‡} and Ling Chen^{*,†}[†]Key Laboratory of Optoelectronic Materials Chemistry and Physics, Fujian Institute of Research on the Structure of Matter, Chinese Academy of Sciences, Fuzhou, Fujian 350002, People's Republic of China[‡]Graduate University of Chinese Academy of Sciences, Beijing 100039, People's Republic of China

Supporting Information

ABSTRACT: New quaternary tellurides, Cs₂Ge₃M₆Te₁₄ (M = Ga, In), were discovered by solid-state reactions. These compounds crystallize in space group *P3̄m1* (No. 164), with *a* = *b* = 8.2475(2) Å, *c* = 14.2734(8) Å, and *V* = 840.82(6) Å³ (*Z* = 1) for Cs₂Ge₃Ga₆Te₁₄ (**1**) and *a* = *b* = 8.5404(2) Å, *c* = 14.6766(8) Å, and *V* = 927.07(6) Å³ (*Z* = 1) for Cs₂Ge₃In₆Te₁₄ (**2**). The remarkable structural feature is the novel three-dimensional [Ge₃M₆Te₁₄]²⁻ anionic framework made by condensed In₆Te₁₄ (or Ga₆Te₁₄) layers that are connected alternately by dimeric Ge³⁺₂Te₆ units and Ge²⁺Te₆ octahedra along the *c* direction. The presence of Ge centers with different oxidation states is also supported by the results of the electron localization function calculation and X-ray photoelectron spectroscopy measurement.

Ternary or quaternary germanium tellurides are interesting because of not only their diverse structural chemistry but also their desired physical properties, which show wide potential applications. For example, Ba₄Ag_{3.95}Ge₂Te₉¹ and Tl₂MGeTe₄ (M = Cd, Hg)² exhibit thermoelectric properties, and M₃GeTe₂ (M = Fe, Ni)³ show magnetic properties. In general, Ge can adopt three different oxidation states in chalcogenides, i.e., Ge²⁺, Ge³⁺, or Ge⁴⁺. Interestingly, each oxidation state has been found in its own distinct local coordination geometry, such as a Ge⁴⁺Q₄ tetrahedron in Li₂CdGeS₄,⁴ K₄Cu₈Ge₃S₁₂,⁵ and Rb₃(AlS₂)₃(GeS₂)₇,⁶ a dimeric Ge³⁺₂Q₆ unit with a covalent Ge–Ge bond in Na₈Sn(Ge₂S₆)₂,⁷ Sr₂Ge₂Se₅,⁸ and Ba₄Ag_{3.95}Ge₂Te₉,¹ and octahedral Ge²⁺Q₆ in Ge₃Sb₂Te₆⁹ and As₄GeTe₇.¹⁰ More interestingly, a few compounds illustrate that Ge atoms with mixed oxidation states can occur in a single compound, such as Tl₂Ge²⁺Ge⁴⁺S₄¹¹ and Ba₂Ge²⁺Ge⁴⁺Se₅.⁸ Moreover, a unique compound, {[Mn(en)₃]₂(Ge₅Te₁₀)_n}, contains multivalent Ge sites, e.g., Ge²⁺, Ge³⁺, and Ge⁴⁺, simultaneously.¹² Besides chalcogenides, the interesting Ge–Ge bonding can also be found in phosphides or halides, such as NaGe₃P₃¹³ and Ge₆Cl₆.¹⁴

To date, quaternary A/Ge/M/Te telluride (A = alkali metals; M = transition metals or main-group metals) remains less explored. Ternary A/Ge/Te tellurides, i.e., K₆Ge₂Te₆,¹⁵ K₂GeTe₄,¹⁶ and Cs₄GeTe₆,¹⁷ are reported. Herein, we report the first quaternary Cs₂Ge₃M₆Te₁₄ [M = Ga (**1**), In (**2**)], which contain both Ge²⁺ and Ge³⁺ centers. These compounds were synthesized from a mixture of 0.6 mmol of M, 0.3 mmol of Ge,

and 1.4 mmol of Te, together with 1.2 mmol of flux CsCl at 820 °C by solid-state reactions. It turned out that CsCl worked as both a flux and a cesium source in these reactions (experimental details are listed in the Supporting Information, SI). X-ray diffraction (XRD) analyses indicated that the yields of the target products (after washing by distilled water) were about 90%, and the minor second phase was Ga₂Te₃ or In₂Te₃. Pure-phased products can be obtained by manually picking crystals (black block crystals; Figure S1 in the SI), and the corresponding XRD patterns are shown in Figures S2 and S3 in the SI. The energy-dispersive X-ray analyses gave stoichiometries of Cs_{1.7(4)}Ge₃Ga_{5.9(4)}Te_{14.2(5)} for **1** and Cs_{1.6(6)}Ge₃In_{6.8(8)}Te_{14.6(7)} for **2**, which are in good agreement with the refined compositions obtained from single-crystal diffraction data (Figures S4 and S5 in the SI).

Cs₂Ge₃M₆Te₁₄ (M = Ga, In) crystallizes in the *P3̄m1* space group, with *a* = *b* = 8.2475(2) Å, *c* = 14.2734(8) Å, and *V* = 840.82(6) Å³ for **1** and *a* = *b* = 8.5404(2) Å, *c* = 14.6766(8) Å, and *V* = 927.07(6) Å³ for **2**. The remarkable structural feature of these compounds is the novel [Ge₃M₆Te₁₄]²⁻ anionic three-dimensional framework made by layers of condensed InTe₄ (or GaTe₄) tetrahedra, which are connected alternately by dimeric (Ge1)³⁺₂Te₆ units and (Ge2)²⁺Te₆ octahedra along the *c* direction (Figure 1).

Each In or Ga atom is coordinated by one Te1, one Te2, and two Te3 atoms in a distorted tetrahedral geometry, as shown in Figure 1, with the M–Te distance varying from 2.6004(9) to 2.6637(7) Å in **1** and from 2.7606(7) to 2.7951(6) Å in **2**, which are comparable with 2.64 Å in Ga₂Te₃¹⁸ and 2.77 Å in AgIn₅Te₈¹⁹ (Table S3 in the SI). Each M₆Te₁₄ layer is constructed of condensed MTe₄ tetrahedra via sharing of 3-fold μ₃-Te2 bridging atoms (shared by three coplanar tetrahedra) and 2-fold μ₂-Te2 bridging atoms (shared by two coplanar tetrahedra); see Figure S6 in the SI. Neighboring M₆Te₁₄ layers are operated to each other by the 3-fold inversion axis located at (0, 0, *z*).

There are two crystallographically independent Ge sites: Ge1 (Wyckoff 2*c* site) and Ge2 (Wyckoff 1*b* site). Ge1 atoms lying at (0, 0, *z*) are dimerized by a covalent Ge1–Ge1 bond (Figure 1, blue bonds), which connect two neighboring M₆Te₁₄ layers via six Ge1–Te1 bonds. The Ge1–Ge1 bond lengths 2.438(2) Å in **1** or 2.432(2) Å in **2** are comparable with 2.45 Å in Tl₆Ge₂Te₆,²⁰ 2.49 Å in K₆Ge₂Te₆,¹⁵ and 2.43 Å in

Received: March 22, 2012

Published: June 15, 2012

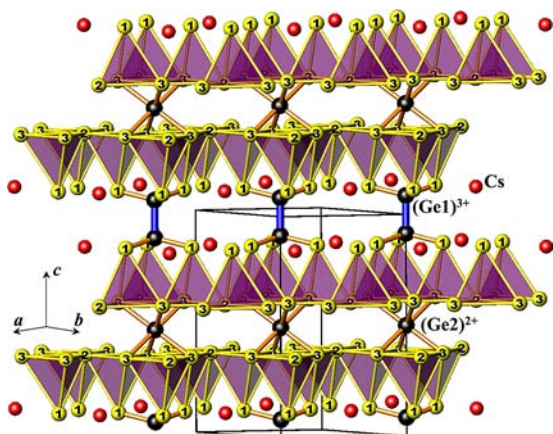


Figure 1. Structure of $\text{Cs}_2\text{Ge}_3\text{M}_6\text{Te}_{14}$ with the Ge1–Ge1 (blue line) and Ge–Te (orange line) bonds outlined. Color code: red, Cs; black, Ge; yellow, Te; purple tetrahedra, MTe_4 ($\text{M} = \text{Ga}, \text{In}$), in which the centering M atoms and M–Te bonds are omitted for clarity.

$\text{Ba}_4\text{Ag}_{3.95}\text{Ge}_2\text{Te}_9$.¹ The Ge1–Te1 bond distances are 2.5671(5) Å in **1** and 2.5842(6) Å in **2**, which are comparable with 2.58 Å in $\text{Ti}_6\text{Ge}_2\text{Te}_6$.²⁰ Differently, Ge2 centers a Ge_2Te_6 octahedron that is constructed of six Te3 atoms, of which three come from the upper layer and three come from the lower one so as to interlink the neighboring M_6Te_{14} layers (Figure 1). The Ge2–Te bond distances 3.0880(5) Å in **1** and 3.0208(5) Å in **2** are comparable with 2.916 Å in As_4GeTe_7 ¹⁰ and 2.993 Å in GeTe .²¹

The Cs^+ cation centers a CsTe_{12} anticubooctahedron constructed of nine Te1 and three Te3 atoms, as shown in Figure S7 in the SI, with Cs–Te distances ranging from 4.1272(2) to 4.4369(2) Å (Table S3 in the SI). These values are comparable to those found in CsTaTe_3 (3.99–4.01 Å),²² CsAuTe (4.02–4.09 Å),²³ and $\text{Cs}_2\text{Mo}_2\text{O}_{14}\text{P}_2\text{Te}$ (4.25–4.44 Å).²⁴

The shortest Te–Te interactions in **1** and **2** are 3.907 and 4.037 Å, which are much longer than the sum of the covalent radius 2.7 Å and are comparable with the sum of the van der Waals radius 4.1 Å; thus, all Te atoms are viewed as Te^{2-} . The $(\text{Ge}1)_2\text{Te}_6$ unit contains a Ge–Ge covalent bond in a typical geometry that is characteristic of the trivalent Ge^{3+} , as reported in $\text{Na}_8\text{Sn}(\text{Ge}_2\text{S}_6)_2$,⁷ $\text{Sr}_2\text{Ge}_2\text{Se}_5$,⁸ and $\text{Ti}_6\text{Ge}_2\text{Te}_6$.²⁰ The formal oxidation state of Ge2 can be assigned as Ge^{2+} according to its octahedral coordination environment, which is the common geometry for the bivalent Ge^{2+} , as found in $\text{Ge}_3\text{Sb}_2\text{Te}_6$ ⁹ and As_4GeTe_7 .¹⁰ Therefore, the charge-balanced formula of **1** and **2** can be described as $\text{Cs}_2\text{Ge}_3\text{M}_6\text{Te}_{14} \equiv (\text{Cs}^+)_2(\text{Ge}1^{3+})_2(\text{Ge}2^{2+})(\text{M}^{3+})_6(\text{Te}^{2-})_{14}$.

The presence of two different oxidation states of Ge (namely, Ge^{2+} and Ge^{3+}) in **1** or **2** can be proven by both the electron localization function (ELF; Figure S8 in the SI) and X-ray photoelectron spectroscopy (XPS) results (Figure 2). Figure S8 in the SI shows the ELF contours of a plane within the $[\text{Ge}_3\text{Ga}_6\text{Te}_{14}]^{2-}$ anion in **1**. The covalent Ge–Ge bond can be clearly seen as the black plane indicated. XPS results of compound **1** indicated the presence of two different binding energies (31.6 and 32.5 eV), which correspond to those of Ge^{2+} and Ge^{3+} , respectively. Furthermore, the $\text{Ge}^{2+}:\text{Ge}^{3+}$ atomic ratio calculated from the area of the XPS peaks is 0.49:1, which agrees well with the 0.5:1 obtained from the single-crystal data refinement.

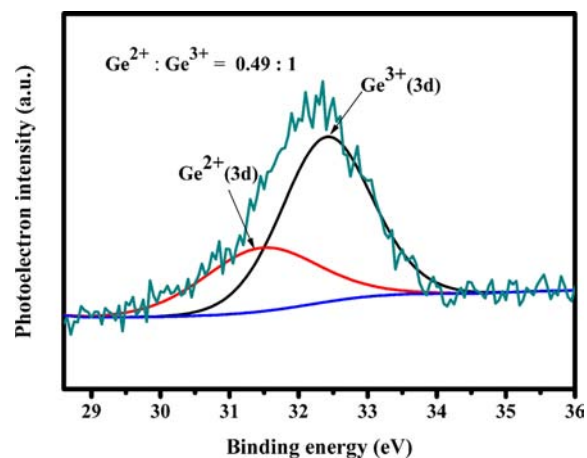


Figure 2. XPS of compound **1**.

To understand the distribution of the states near the Fermi level, the densities of states (DOS) of **1** and **2** were calculated (Figures 3a and S9 in the SI). The valence band (VB) near the Fermi level is dominated by the Ga 4p, Ge 4p, and Te 5p states, whereas the conduction band (CB) has most of its contributions coming from Te 5p, Ge 4s, Ga 4s, Ge 4p, and Ga 4p with minor Cs 6s and Cs 5p contributions. In the band structure of **1**, the VB maximum and CB minimum locate at

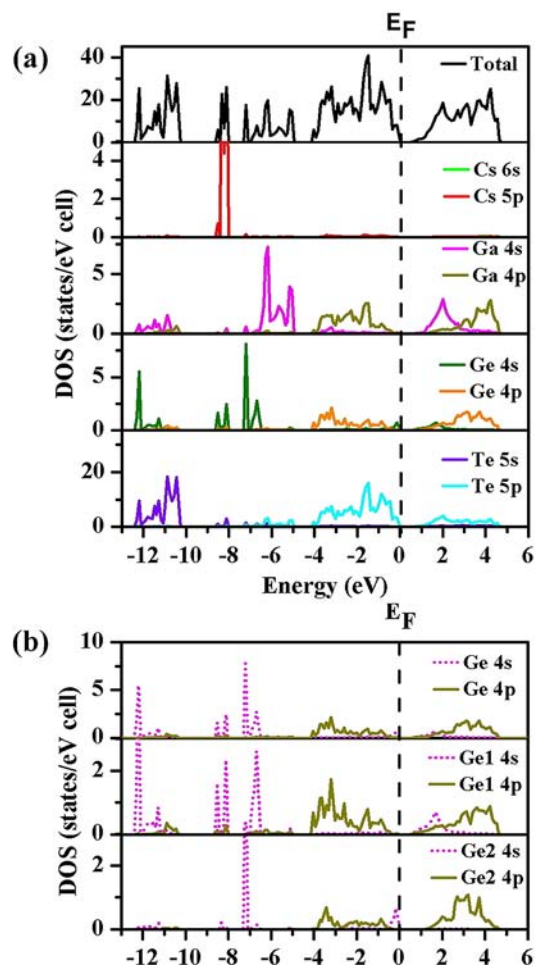


Figure 3. (a) Total and partial DOSs of **1**. (b) Enlarged DOSs of Ge1 and Ge2.

different k points, indicating a computational indirect narrow band of about 0.53 eV (Figure S10 in the SI). Compound **2** has a similar band structure but a slightly larger computational band gap of about 0.63 eV (Figure S11 in the SI). According to the DOSs, $(\text{Ge}1)^{3+}$ has less 4s states below E_F than $(\text{Ge}2)^{2+}$ does because some $(\text{Ge}1)^{3+}$ 4s states distribute above E_F , whereas $(\text{Ge}2)^{2+}$ 4s states almost distribute below E_F (Figure 3b).

In conclusion, the first two quaternary three-dimensional telluride frameworks, $\text{Cs}_2\text{Ge}_3\text{M}_6\text{Te}_{14}$ ($M = \text{Ga}, \text{In}$), with Ge in different oxidation states in the A/Ge/M/Te system ($A =$ alkali metals; $M =$ transition metals or main-group metals), have been discovered. The presence of Ge^{3+} and Ge^{2+} is revealed by characteristic coordination geometries around Ge centers according to the single-crystal diffraction data, as well as the results of the ELF calculation and XPS measurement. The primary electron structure analyses indicate small-band-gap semiconducting nature of these compounds, and further investment on their physical properties is worth trying.

■ ASSOCIATED CONTENT

📄 Supporting Information

CIF data, experimental and theoretical methods, and additional tables and figures. This material is available free of charge via the Internet at <http://pubs.acs.org>.

■ AUTHOR INFORMATION

Corresponding Author

*E-mail: chenl@fjirms.ac.cn. Tel: (011)86-591-83704947.

Notes

The authors declare no competing financial interest.

■ ACKNOWLEDGMENTS

This research was supported by the National Natural Science Foundation of China under Projects 90922021, 20973175, and 21171168 and the “Knowledge Innovation Program of the Chinese Academy of Sciences” (Grant KJCX2-YW-H20).

■ REFERENCES

- (1) Cui, Y. J.; Assoud, A.; Kleinke, H. *Inorg. Chem.* **2009**, *48*, 5313.
- (2) McGuire, M. A.; Scheidemantel, T. J.; Badding, J. V.; DiSalvo, F. *J. Chem. Mater.* **2005**, *17*, 6186.
- (3) Deiseroth, H. J.; Aleksandrov, K.; Reiner, C.; Kienle, L.; Kremer, R. K. *Eur. J. Inorg. Chem.* **2006**, 1561.
- (4) Lekse, J. W.; Moreau, M. A.; McNerny, K. L.; Yeon, J.; Halasyamani, P. S.; Aitken, J. A. *Inorg. Chem.* **2009**, *48*, 7516.
- (5) Zhang, R. C.; Yao, H. G.; Ji, S. H.; Liu, M. C.; Ji, M.; An, Y. L. *Inorg. Chem.* **2010**, *49*, 6372.
- (6) Rothenberger, A.; Shafaei-Fallah, M.; Kanatzidis, M. G. *Inorg. Chem.* **2010**, *49*, 9749.
- (7) Marking, G. A.; Kanatzidis, M. G. *J. Alloys Compd.* **1997**, *259*, 122.
- (8) Johrendt, D.; Tampier, M. *Chem.—Eur. J.* **2000**, *6*, 994.
- (9) Matsunaga, T.; Kojima, R.; Yamada, N.; Kifune, K.; Kubota, Y.; Takata, M. *Appl. Phys. Lett.* **2007**, *90*, 161919.
- (10) Shu, H. W.; Jaulmes, S.; Flahaut, J. *J. Solid State Chem.* **1988**, *74*, 277.
- (11) Eulenberger, G. *J. Less-Common Met.* **1985**, *108*, 65.
- (12) Zhang, Q. C.; Armatas, G.; Kanatzidis, M. G. *Inorg. Chem.* **2009**, *48*, 8665.
- (13) Feng, K.; Yin, W. L.; He, R.; Lin, Z. S.; Jin, S. F.; Yao, J. Y.; Fu, P. Z.; Wu, Y. C. *Dalton Trans.* **2011**, *41*, 484.
- (14) Beattie, I. R.; Jones, P. J.; Reid, G.; Webster, M. *Inorg. Chem.* **1998**, *37*, 6032.
- (15) Dittmar, G. Z. *Anorg. Allg. Chem.* **1979**, *453*, 68.

- (16) Eisenmann, B.; Schrod, H.; Schäfer, H. *Mater. Res. Bull.* **1984**, *19*, 293.
- (17) Brinkmann, C.; Eisenmann, B.; Schäfer, H. *Mater. Res. Bull.* **1985**, *20*, 1207.
- (18) Julien-Pouzol, M.; Jaulmes, S.; Alapini, F. *Acta Crystallogr., Sect. B* **1977**, *33*, 2270.
- (19) Mora, A. J.; Delgado, G. E.; Pineda, C.; Tinoco, T. *Phys. Status Solidi A* **2004**, *201*, 1477.
- (20) Eulenberger, G. *J. Solid State Chem.* **1984**, *55*, 306.
- (21) Parker, S. G.; Pinnell, J. E.; Swink, L. N. *J. Mater. Sci.* **1974**, *9*, 1829.
- (22) Pell, M. A.; Vajenine, G. V. M.; Ibers, J. A. *J. Am. Chem. Soc.* **1997**, *119*, 5186.
- (23) Bronger, W.; Kathage, H. U. *J. Alloys Compd.* **1992**, *184*, 87.
- (24) Guesdon, A.; Raveau, B. *Chem. Mater.* **2000**, *12*, 2239.